



OPEN

One-year longitudinal study of the stratum corneum proteome of retinol and all-*trans*-retinoic acid treated human skin: an orchestrated molecular event

Kahina Abed^{1✉}, Aude Foucher¹, Dominique Bernard¹, Emmanuelle Tancrède-Bohin^{1,2,3} & Nükhet Cavusoglu^{1,3}

Topically applied all-*trans*-retinoic acid (RA) is a gold-standard anti-aging molecule used in dermatology. As its cosmetic counterpart used in anti-aging, Retinol (ROL) is also a known metabolic precursor of RA. Despite this metabolic link, they haven't been compared exhaustively in vivo at a mechanistic level. Therefore, to highlight the effect of a topical application of both molecules on in vivo skin, we undertook a longitudinal 1-year study and performed an untargeted proteomic analysis to get a more holistic view on the underlying biological mechanisms of action. The generation of the temporal proteomics signatures of retinol and all-*trans*-retinoic acid reveals the impact of these molecules on biological functions related to the aging of skin. New biological functions impacted by retinoids were discovered: glycan metabolism and protein biosynthesis. In addition, the temporal analysis reveals highest modulations at early time points while the physical measures, such as epidermal thickening, was mostly observed at the latest time point, demonstrating a strong time lapse between molecular and morphological impacts. Finally, these global temporal signatures could be used to identify new cosmetic compounds of interest.

Skin aging is a complex process that is a consequence of genetic and environmental interactions. While chronological aging is relentless, the biological and physical results of chronological aging vary in their kinetics, biological events, and clinical manifestations.

Since clinical changes in skin are among the most visible signs of aging, skin appearance has a significant emotional and psychological impact on our quality of life. As well as appearance, skin aging has a significant impact on age-related skin diseases, notably impaired wound healing in the elderly suggesting a dysregulation of molecular mechanisms during the aging process¹⁻⁴. In particular, skin proteome has been shown to be altered during aging⁵.

Topical All-*trans*-retinoic acid (RA), used in dermatology for its benefits in the treatment of acne as well as for various keratinization and pigmentation disorders, is the gold-standard treatment prescribed by dermatologists for treating photodamaged skin⁶⁻⁸. Topical retinol (ROL), its precursor, has also been used for decades in topical anti-aging cosmetics⁹. While their impact on aging's clinical, immuno-histochemical or molecular parameters have been extensively studied, the molecular mechanisms of action of ROL and RA in a temporal manner remains unexplored.

To fill this knowledge gap, we followed the molecular events taking place in the *stratum corneum* (SC) after topical application of ROL and RA over the course of 1 year. We used a state-of-the-art proteomic approach, combining liquid chromatography-tandem mass spectrometry (LC-MS/MS) and isobaric markers for relative quantification, to produce to our knowledge the first in vivo temporal signature of ROL and RA topical application on in vivo skin.

¹L'Oréal Research and Innovation, Aulnay-Sous-Bois, France. ²Service de Dermatologie, Hôpital Saint-Louis, Paris, France. ³These authors contributed equally: Emmanuelle Tancrède-Bohin and Nükhet Cavusoglu. ✉email: Kahina.abed@loreal.com

Materials and methods

Clinical study. The clinical study was conducted in Paris, France, between February 2011 and April 2012, and the experimental protocol was approved by the Saint Louis Hospital ethics committee (EC reference 2010/58), complying with the Declaration of Helsinki and all volunteers gave written informed consent. Clinical and epidermal changes including morphology, melanin content and distribution assessed by histology and *in vivo* multiphoton microscopy have already been published¹⁰.

This study involved 30 female volunteers (50–65y) with constitutive skin color determined by ITA value between 10° and 41° (ITA group III/IV). They applied Retinol 0.3% (ROL 0.3% cream, L'Oréal group) (n = 15) or all-*trans*-Retinoic acid 0.025% (RA 0.025% cream, Galderma) (n = 15) on one dorsal forearm versus a control product (white paraffin containing excipient, Bayer) on the other forearm for 1 year.

Non-invasive strippings (D-squams[®]) were performed on the treated and non-treated arms at 3 months (June), 6 months (September), and 12 months (March + 1 yr), for each volunteer. These groups were further divided in three sub-groups for ROL treated and 3 sub-groups for the ROL control group before iTRAQ labeling of each sub-group, thus giving a triplex experiment of each condition. The same design was applied for the RA treatment (Fig. 1).

Areas of investigation were identified by tracing on transparent plastic sheets (Monaderm, Monaco) natural anatomic marks (external and internal forearm edges, ulna head, elbow fold) and also skin folds and neavus on volunteers in a standardized position.

Protein extraction, iTRAQ labeling and mass spectrometry analysis. Protein extractions were performed from each individual from D-squams[®] strippings as published earlier¹¹. Briefly, proteins were extracted in a deoxycholate buffer using mechanical lysis. After precipitation in 4 volumes acetone, proteins were resolubilized, reduced by TCEP and alkylated using methyl methanethiosulfonate (MMTS) prior to digestion by trypsin.

Tryptic peptides were labeled using iTRAQ 4 plex reagent before desalting. Fractionation of the peptides was performed in gel using isoelectric focusing on a 3–10 pH gradient gel strip to generate *in fine* 18 fractions. Each fraction was analyzed by mass spectrometry on a 5600 Triple-TOF (ABSciex, Framingham, USA) coupled to an HPLC (Agilent 1200). The experimental design permitted three independent LC-MS/MS analyses. Briefly 500 ng of samples were injected onto a trapping column for desalting followed by a chromatographic separation (nanoLC) on a 75 µm ID x 15 cm with particle size of 5µm Reverse Phase (RP) C18 column. Samples were run using a 90 min gradient from 10 to 35% solvent B (solvent A being a solution of 0.1% formic acid and solvent B: 0.1% formic acid in acetonitrile) at a flow rate of 300 nl/min. Data were acquired using a positive ESI mode with

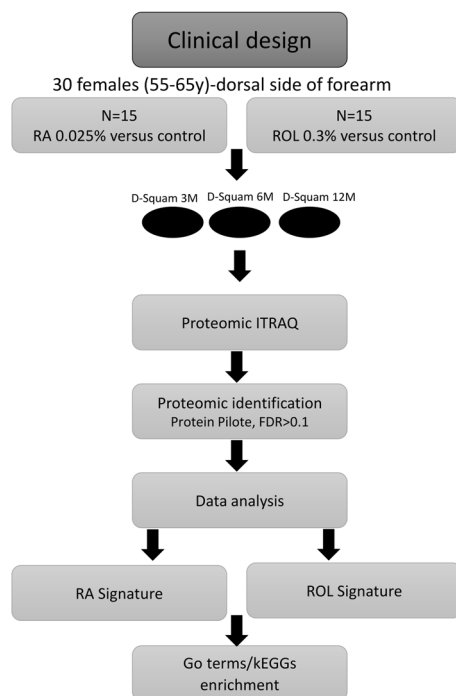


Figure 1. Scheme of overall Clinical and analytical design of the study. The clinical study was carried out on a total of 30 subjects, 15 of whom received a daily application of RA at 0.025% and 15 others of ROL at 0.3%. Samplings were carried out at 3 months (3 M), 6 months (6 M) and 12 months (12 M). Protein extractions were performed from everyone from D-squams[®]. Each iTRAQ (isobaric Tags for Relative and Absolute Quantitation) experiment allowed the comparison of a group treated with RA against the same group control, and a group treated with ROL against the same group control.

a voltage of 2.4 kV in positive mode. Full scans were obtained in the mass range of 400–1250 in 250 ms. Data dependent acquisition (DDA) was used for data collection for the high intensity ions in the m/z range 100–1600.

Protein identification. Data files were submitted for simultaneous searches using Protein Pilot version 4.0 software (AB Sciex) and Mascot search engine (Matrix Science) with the following criteria: Trypsin digestion, fixed modification on cysteine of methylthio, variable modification iTRAQ (4 plex iTRAQ (K), iTRAQ (N-term), iTRAQ (Y)) and methionine oxidation. Peptide charge was restricted to +2, +3 and +4. Peptide mass tolerance restricted to or set at (± 0.1) and fragment mass tolerance was ± 0.1 . Proteins were defined as differentially modulated if they fit the following criteria: at least two peptides with high confidence (95%) for identification (p -value < 0.05) and with a fold change of proteins greater or equal to $|1.5|$.

ELISA. Sandwich ELISA assay was performed to quantify transglutaminase 3 (TGM3) using an in-house developed assay using Meso Scale technology (Meso Scale Discovery). Custom made HuCal (human combinatorial antibody library) antibodies were developed by AbD Serotec BioRad for these ELISAs. For TGM3 ELISA, standard curve was produced using recombinant TGM3 (Zedira, #T024), capture antibody (HuCal_AbD12765) and detection antibody (HuCal_AbD12866). An 8 points standard curve (0–0.5 mg/ml (0.0075, 0.0156, 0.0313, 0.0625, 0.125, 0.25, 0.5)) was made in triplicate. Samples were diluted 1/5 in MSD sample diluent and 25 μ l was loaded per well. Detection was performed using anti-species sulfo-tagged antibodies from Meso Scale Discovery. Plates were read in a MesoSector S6000 plate reader (Meso Scale Discovery).

Data analysis. Differentially expressed proteins of retinoids treated subject and vehicle subject, were defined by a fold change $\geq |1.5|$ in 2 or 3 replicates. The biological interpretation of these protein lists was performed by enrichment calculations using the R ClusterProfiler package¹² and by using the "Gene Ontology" databases¹³. A term from Gene Ontology or a Pathway from the KEGG database was significantly impacted when it had a corrected p -value < 0.05 with the list of proteins given as input¹⁴. Heatmap or volcano plot type visualizations were also generated with the R tool to facilitate visualization and biological interpretation of the results.

Results

To investigate the molecular mechanisms by which topical application of ROL or RA acts on the skin, we used an iTRAQ based proteomics approach to highlight all the proteins and therefore functions involved in those mechanisms. ROL and RA were applied daily on the dorsal photodamaged forearm over 1 year and samples were taken at 3, 6 and 12 months.

Global analysis of differentially expressed proteins (DEPs) revealed a high impact of ROL and RA application on skin's surface proteome. In summary, 217 proteins (106 upregulated and 111 downregulated) (Fig. 2a) and 219 (106 upregulated and 113 downregulated) (Fig. 2b) were modulated by ROL and RA, respectively. 141 DEPs were modulated by the topical application of both retinoids (65%) and defined the biological signature of each of the retinoids (Fig. 2c).

As a preliminary validation, we focused on two well-known characterized binding proteins shown to bind RA and deliver it to the receptors, FABP5 (Fatty Acid Binding Protein 5) and CRABP2 (Cellular Retinoic Acid Binding Protein 2)^{15,16}. Both were upregulated in this study with a fold change up to 8.

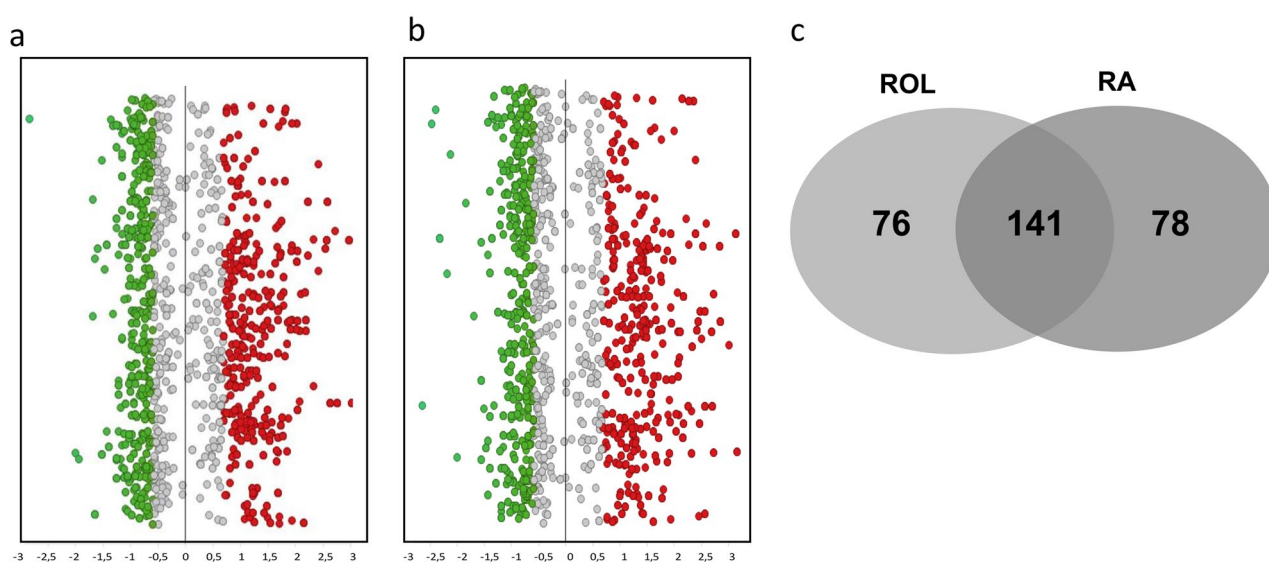


Figure 2. Visualization of DEPs after ROL (a) and RA (b) treatment. Distribution of protein based on log₂-transformed fold change. Red dots indicate upregulated proteins, green dots indicate downregulated proteins and grey dots represents not modulated proteins. (c) Venn diagram representation of the differentially modulated proteins by ROL and RA treatment.

Macroscopic analysis of retinoids signatures revealed similar biological impacts in terms of protein levels and their direction of modulation. This is exemplified in the radar plot, showing the 42 DEPS common to ROL and RA at 12 months (Fig. 3).

Similar global biological impact of ROL and RA. To elucidate the biological processes and metabolic pathways that are affected by the application of ROL and RA, we performed a Gene Ontology (GO) term and KEGG pathway enrichment analysis on the signatures obtained from the combined time points 3, 6 and 12 months. As expected, no specific biological processes to ROL or RA have been identified (Fig. 4).

To create a meaningful analysis, we condensed the numerous biological processes into 7 superpathways (Table 1) which covered: energy/canonical glycolysis, antimicrobial response, anti-oxidative defense, epidermal barrier-associated proteins, glycan metabolism, cytoskeletal rearrangement, and protein assembly/folding.

These 7 superpathways were then utilized to evaluate the biological impacts of the retinoids on the skin's biology and the adaptability of the SC to their application through the temporal signatures. Combining the biological functions with the temporal signature, we were able to define the orchestrated molecular events detected in the SC which reflected what was occurring in the epidermis.

Temporal evolution of ROL and RA proteomic signatures. Temporal signatures were obtained by plotting the number of DEPs at each time point of the analysis. This visualization shows the rapid decline of DEPs impacted by ROL and RA treatment (Fig. 5). To our knowledge, this in vivo temporal signature demonstrates for the first time the evolution in the biological skin response to retinoids treatment.

To determine if this global trend was similar for all the biological functions, we analyzed the evolution of each superpathway independently (Fig. 6).

The evolution curves can be classified in three profiles: 1- decreasing temporal signature containing up and down DEPs (i.e.: antimicrobial response, anti-oxidative defense), 2- decreasing temporal signature containing proteins with a similar modulation (energy/canonical glycolysis, cytoskeletal rearrangement, and protein assembly/folding), 3- pathway with stable temporal effect (epidermal barrier-associated protein). For interpretation of the biological impact, we have focused on profiles 2 and 3.

Early increase of energy production, protein assembly/folding and cytoskeletal rearrangement by ROL and RA. *Energy/canonical glycolysis.* The glycolysis pathway exhibited significant modulation by retinoids with six enzymes upregulated and one enzyme downregulated, among the 10 enzymes comprising this pathway. At 3 months of application GPI (Glucose-6-Phosphate-isomerase; FC ROL = 1.9, RA = 2.8), ALDOA (Fructose biphosphate aldolase A FC ROL = 2.4, RA = 2.4), PGK1 (phosphoglycerate kinase

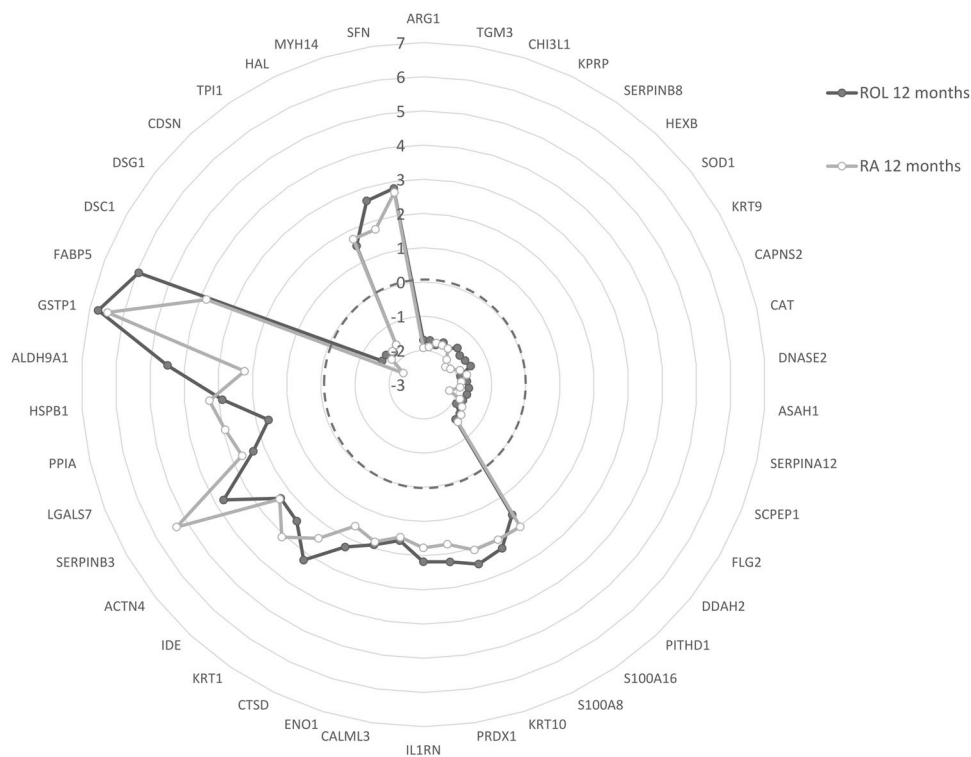


Figure 3. Radar plot representation of the 42 DEPs common to ROL (Black, filled circles) and RA treatments (grey, empty circles) at 12 months. Proteins are identified with their Gene Names. The axis indicates the fold change, while the dotted circle delimitates the up- and downregulated proteins.

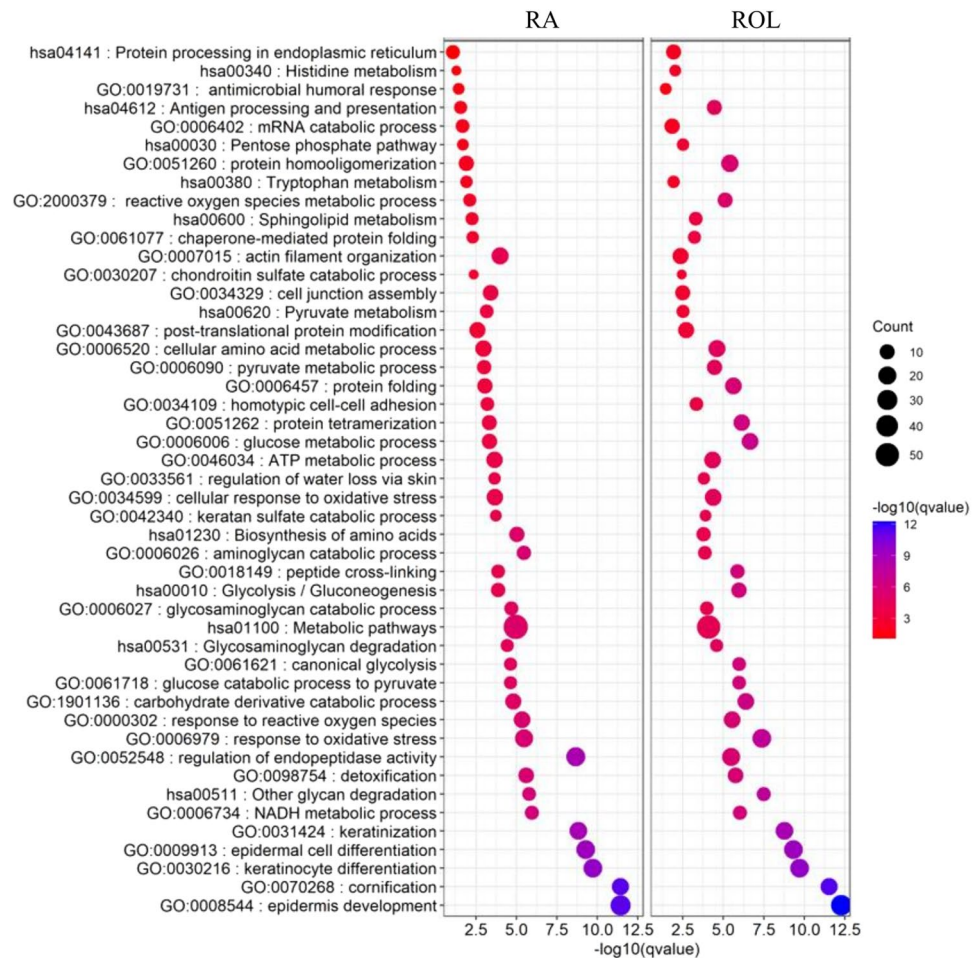


Figure 4. Dotplot representation of selected enriched biological processes and KEGG pathways for RA (left panel) and ROL (right panel). The size of the dots represents the number of proteins implicated in the enrichment. The color code of the dots represents the adjusted p -values of the enrichment in $-\log_{10}(q\text{value})$.

1 FC ROL = 2.2, RA = 2.2), PGAM1 (phosphoglycerate mutase 1 FC RA = 2.4), ENO1 (enolase FC ROL = 2.1, RA = 1.6), and Phosphoglycerate kinase 1 (PGK1 FC RA = 2.1) were upregulated. Interestingly the early time points 3 and 6 months showed the most important increase in these enzymes (Figs. 7 and 8a).

Protein assembly/folding. The protein synthesis/folding was enhanced after both treatments with 16 upregulated proteins for ROL and 11 upregulated proteins for RA. The orchestrated molecular events can be defined by the early increase of translation initiation factors EIF2S1 (Eukaryotic translation initiation factor 2 subunit 1), EIF6 (Eukaryotic translation initiation factor 6) and EIF4A1 (Eukaryotic initiation factor 4A-I) at 3 months followed by the subsequent increase in the elongation process factor EEF2 (Eukaryotic translation elongation factor 2) at 6 month (RA) and 12 months (ROL) (Fig. 8b).

Cytoskeletal rearrangement. Twenty-one proteins found upregulated by ROL and RA were involved in cytoskeletal rearrangement (Fig. 8c) (18/21 by ROL and 17/21 by RA), with the greatest DEPs observed at 3 months. Among them we identified three protein families, the actinin family proteins ACTN4 (Actinin Alpha 4) and ACTG1 Actin Gamma 1), the myosin superfamily proteins MYH9 (Myosin-9) and MYH14 (Myosin-14), and the 14-3-3 family proteins YWHAG (14-3-3 protein gamma) and YWHAZ (14-3-3 protein zeta/delta). Once again, the protein levels exhibited the most important increases at the early time points of 3 and 6 months.

Decreased glycan metabolism by ROL and RA. A large impact of ROL and RA was observed on glycan metabolism with 14 glycosidases downregulated at 3 months (Fig. 8d). These enzymes are known to be mainly involved in the de-glycosylation of several types of glycans: N-glycans, O-glycans, heparan sulfate, dermatan sulfate, chondroitin sulfate and keratan sulfate (Fig. 9). Comparison of ROL and RA signatures on glycan metabolism revealed some differential impact of the retinoids.

| Superpathways | Selected enriched go and kegg terms |
|--------------------------------------|---|
| Energy/canonical glycolysis | GO:0061621/canonical glycolysis |
| | GO:0061718/glucose catabolic process to pyruvate |
| | GO:1901136/carbohydrate derivative catabolic process |
| | GO:0006006/glucose metabolic process |
| | GO:0046034/ATP metabolic process |
| | GO:0006090/pyruvate metabolic process |
| | GO:0006734/NADH metabolic process |
| | hsa00010/Glycolysis |
| | hsa00620/Pyruvate metabolism |
| | hsa00030/Pentose phosphate pathway |
| Antimicrobial response | GO:0019730: antimicrobial humoral response |
| Anti-oxidative defense | GO:0034599/cellular response to oxidative stress |
| | GO:2000379/ reactive oxygen species metabolic process |
| | GO:0000302/response to reactive oxygen species |
| | GO:0098754/detoxification |
| | GO:0006979/response to oxidative stress |
| Epidermal barrier-associated protein | GO:0008544/epidermis development |
| | GO:0033561/regulation of water loss via skin |
| | GO:0052548/regulation of endopeptidase activity |
| | GO:0018149/peptide cross-linking |
| | GO:0031424/keratinization |
| | GO:0009913/epidermal cell differentiation |
| | GO:0030216/keratinocyte differentiation |
| | GO:0070268/cornification |
| hsa00600/Sphingolipid metabolism | |
| Glycan metabolism | GO:0006027/glycosaminoglycan catabolic process |
| | GO:0030207/chondroitin sulfate catabolic process |
| | GO:0006026/aminoglycan catabolic process |
| | GO:0042340/keratan sulfate catabolic process |
| | hsa00511/Other glycan degradation |
| | hsa00531/Glycosaminoglycan degradation |
| | hsa01100/Metabolic pathways |
| Cytoskeletal rearrangement | GO:0007015/actin filament organization |
| | GO:0034329/cell junction assembly |
| | GO:0034109/homotypic cell–cell adhesion |
| Protein assembly/folding | GO:0006402/mRNA catabolic process |
| | GO:0043687/post-translational protein modification |
| | GO:0061077/chaperone-mediated protein folding |
| | GO:0006520/cellular amino acid metabolic process |
| | GO:0051260/protein homooligomerization |
| | GO:0006457/protein folding |
| | GO:0051262/protein tetramerization |
| | hsa04612/Antigen processing and presentation |
| | hsa01230/Biosynthesis of amino acids |
| | hsa00340/Histidine metabolism |
| | hsa00380/Tryptophan metabolism |
| | hsa04141/Protein processing in endoplasmic reticulum |

Table 1. List of the 7 superpathways created from selected biological processes and KEGG pathways.

Notably, five enzymes were specifically downregulated by ROL: GAA (acid alpha-glucosidase), GALNS (galactosamine-6-sulfate sulfatase), GBA (glucosidase beta acid), MAN2B2 (mannosidase alpha class 2B member 2) and NAGA (N-acetylgalactosaminidase alpha).

Long lasting impact of ROL and RA on epidermal barrier-associated proteins. The epidermal barrier-associated proteins related to the eponym function were strongly impacted by ROL and RA application at all time points. This observation suggested a long-lasting effect of the retinoids on these proteins and required

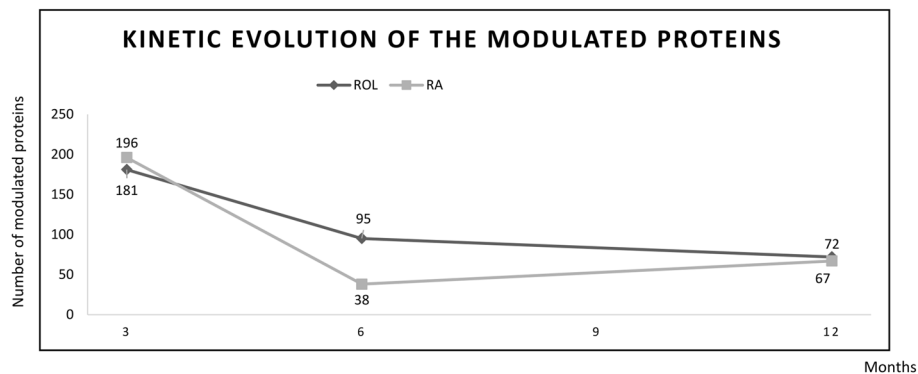


Figure 5. Evolution of the number of modulated proteins over time (months) for ROL (black) and RA (grey).

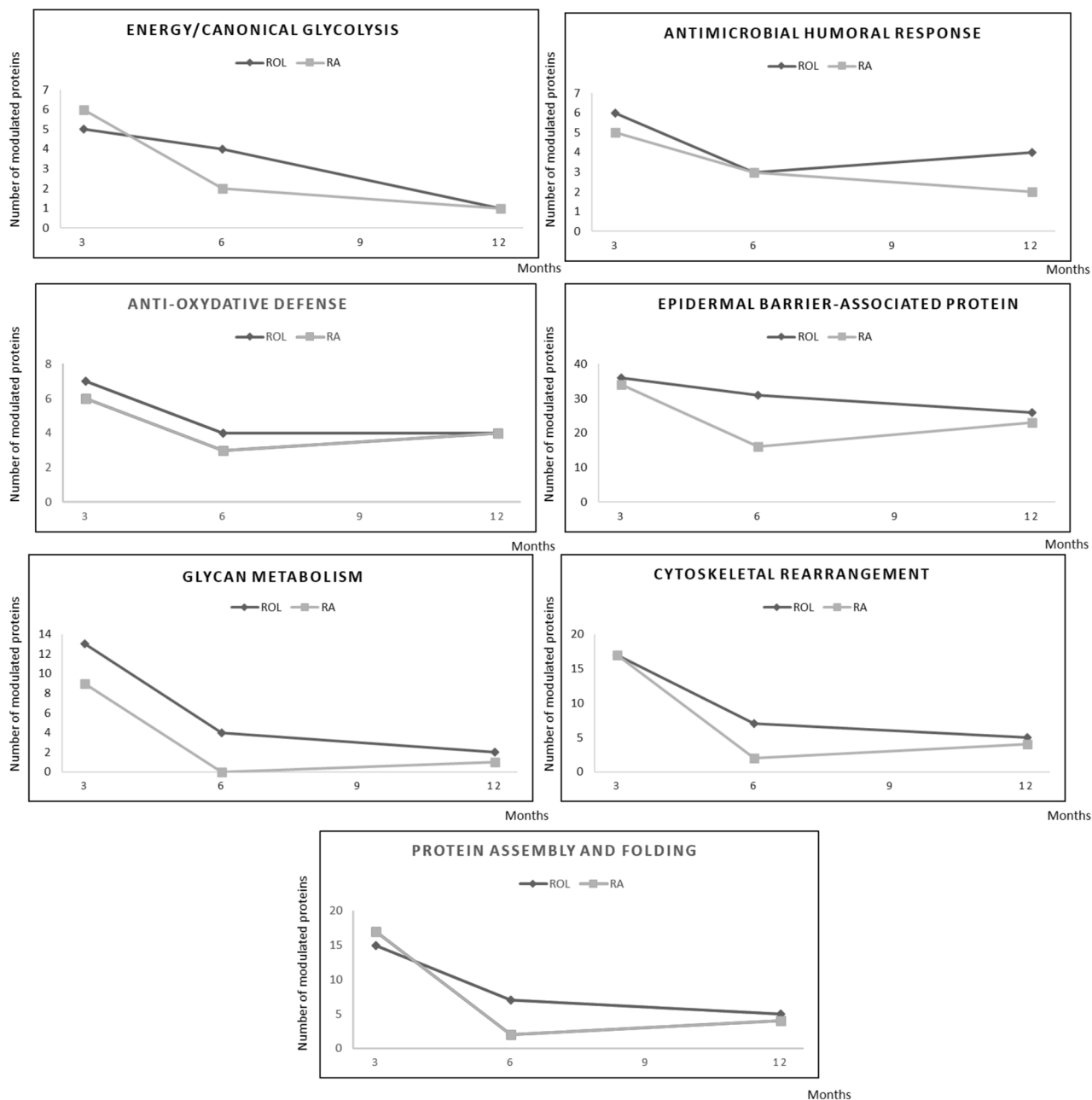


Figure 6. Evolution of the number of DEPs in the 7 superpathways for ROL (black) and RA (grey).

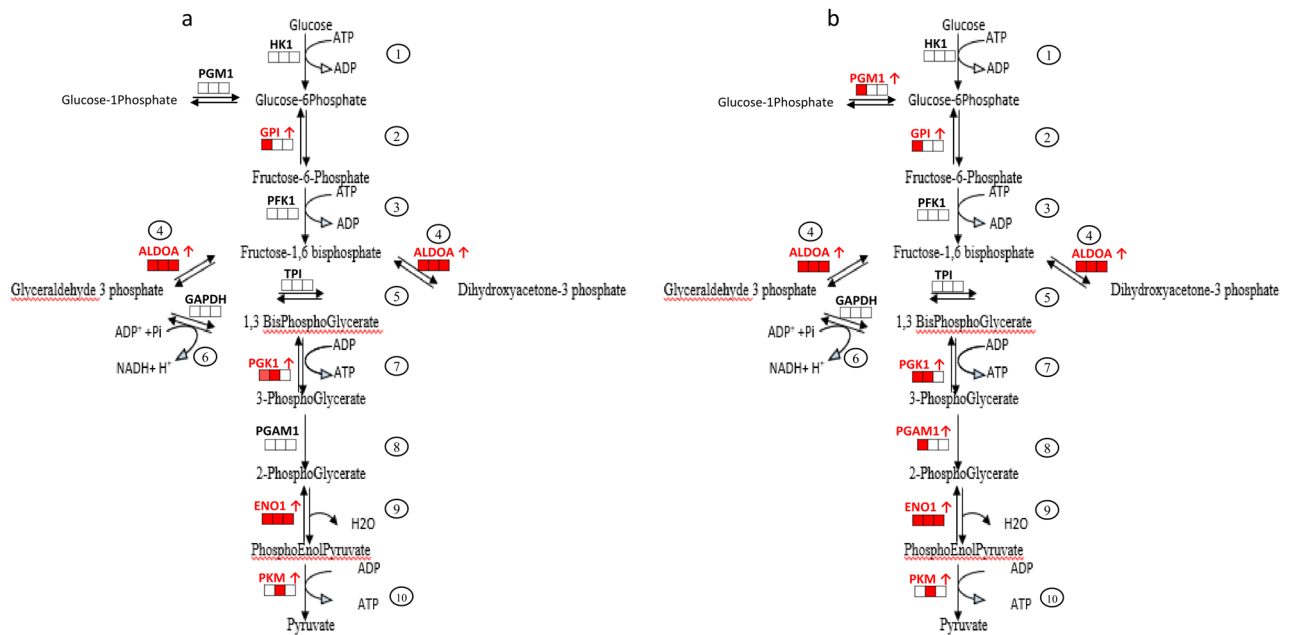


Figure 7. Impact of ROL (a) and RA (b) application on enzymes of the glycolysis metabolic pathways at 3, 6, and 12 months. Each square represents the up- (red) or non- modulation (white) of the enzymes at 3 (left square), 6 (middle square) and 12 (right square) months.

further description. 53 DEPs belonged to this superpathway and covered the following functions: ‘cornified envelope components’, ‘Ca²⁺-binding S100 protein family’, ‘intermediate filament’, ‘lipid metabolic process’, ‘serine protease and protease inhibitors’, and ‘desmosome’. Except for desmosome proteins which were all down-regulated, and ‘Ca²⁺-binding S100 protein family’ in which all proteins were upregulated, the other functions showed a mixed protein dynamic (Fig. 8e).

A marked dysregulation of numerous keratins was observed after treatment by both retinoids: upregulation of KRT1 (Keratin 1), KRT4 (Keratin 4) and KRT10 (Keratin 10) and downregulation of KRT2 (Keratin 2) and KRT9 (Keratin 9). Some specificity of ROL and RA was also observed with ROL (Keratin 5 (KRT5) and KRT14 (Keratin 14)) or RA (KRT15 (Keratin 15)).

In cornified envelope function, FLG (Filaggrin), IVL (Involucrin), PPL (Periplakin), KRTDAP (keratinocyte differentiation-associated protein), and CALML3 (calmodulin-like protein 3) were upregulated by both retinoids while EVPL (envoplakin) was only upregulated by ROL. Additionally, transglutaminase enzymes TGM1 (transglutaminase 1) and TGM3 were downregulated at all time points, which was confirmed for TGM3 by ELISA (Table 2).

Proteins associated with lipid metabolism and signaling showed a strong upregulation for FABP5 (FC = 8,8) with ROL and RA, in contrast to a downregulation of eight proteins involved in ceramide synthesis such as ASAH1 (Acid ceramidase) and in cholesterol synthesis as seen for ACAT2 (acetyl-CoA acetyltransferase 2).

Discussion

This study brings the first temporal *in vivo* proteomic signatures of ROL (217 proteins) and RA (219 proteins) in the SC with a proteomic analysis strategy based on iTRAQ quantitative proteomic to compare the effect of ROL and RA daily application on skin in a long-term study. The comparison of the two signatures revealed: (1) a high homology between ROL and RA effects (65% of DEPs were in common), (2) the same biological functions impacted and (3) a similar evolution pattern of skin’s molecular response over time which is not surprising knowing that ROL is the metabolic precursor of RA. As it is well known that for comparable concentrations, RA is more effective and more irritating than ROL, we used a much higher concentration of ROL than RA in this study ($\times 12$). We analyzed the data as a comprehensive retinoid signature taking into account the substantial difference in concentration. Consequently, any comparison between the 2 actives will be made in the context of this significant difference in concentration. We will first focus on the known and new biological functions impacted by retinoids and then on the temporal aspect of the skin’s molecular response.

Since retinoids are known for their effect on aging signs, we will focus on deciphering the molecular mechanisms leading to anti-aging benefits. One of the best-known hallmarks of aging is the decrease in energy production^{17,18}. In our study, energy production was boosted by retinoids¹⁹ through the upregulation of 5 essential enzymes (ENO1, PGM1 (Phosphoglucomutase 1), PGK1, PKM (Pyruvate kinase M1/2), and GPI) of the glycolysis pathway. This hypothesis can be supported by the finding of Ahmad Alatshan et al.²⁰ which showed that RA increases the metabolic pathways towards glycolysis.

Another hallmark of aging is the imbalance of proteostasis¹⁸, which in skin can be characterized by the balance in proliferation/differentiation of epidermal keratinocytes²¹. An increase in the proliferation of epidermal

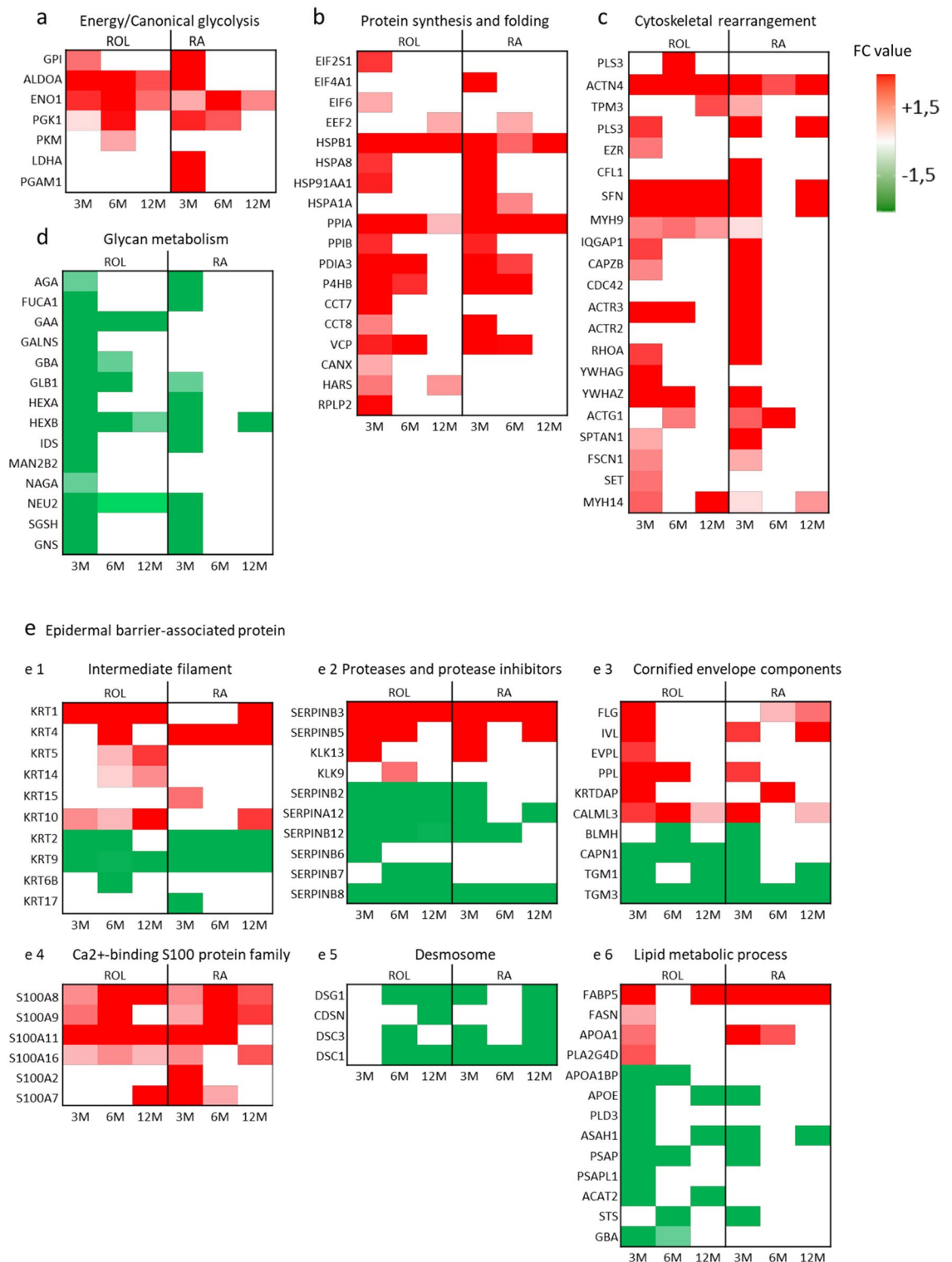


Figure 8. Heatmap of fold-change values of DEPs during ROL and RA treatment for each superpathway. (a) Energy/canonical glycolysis, (b) Protein assembly/folding, (c) Cytoskeletal rearrangement, (d) Glycan metabolism (e) Epidermal barrier-associated protein: (e1) Intermediate filament, (e2) Proteases and protease inhibitors, (e3) Cornified envelope components, (e3) Ca²⁺-binding S100 protein family, (e4) Desmosome, and (e5) Lipid metabolic process. Horizontal axis: time points 3 months (3 M), 6 months (6 M) and 12 months (12 M). Color key: Green denotes downregulation while red denotes upregulation.

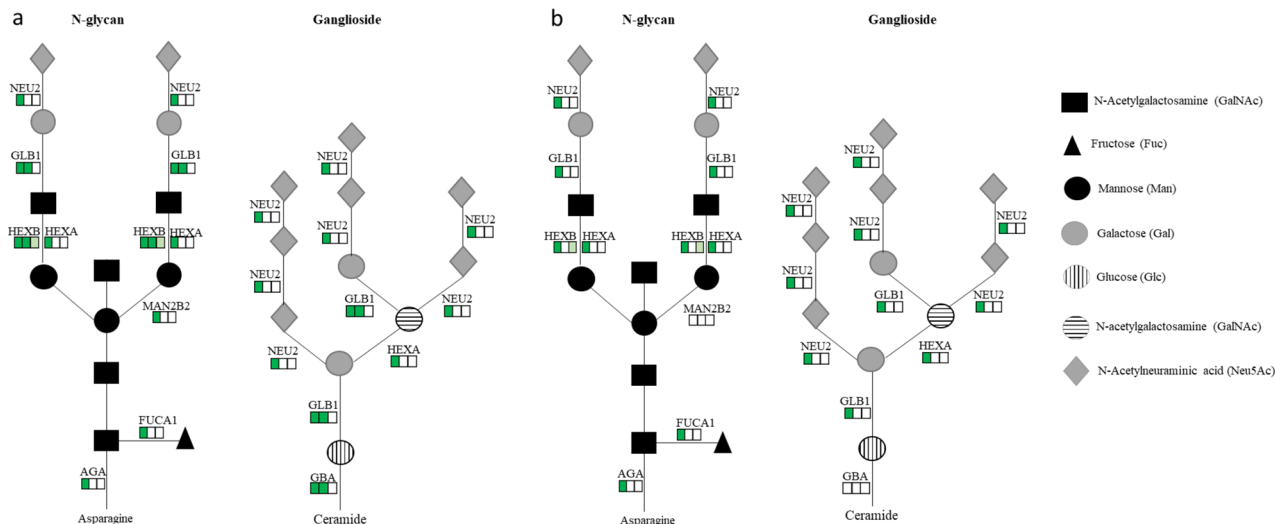


Figure 9. Glycosaminoglycan degradation with the projection of the modulation of the enzymes by ROL (a) and RA (b). Each square represents the down- (green) or non- modulation (white) of the enzymes at 3 (left square), 6 (middle square) and 12 (right square) months.

| TGM3 | 3 Months | | 6 Months | | 12 Months | |
|----------------|----------|-----------------|----------|-----------------|-----------|-----------------|
| | Ratio | <i>P</i> -value | Ratio | <i>P</i> -value | Ratio | <i>P</i> -value |
| ROL vs vehicle | 0.6 | 0.22 | 0.87 | 0.68 | 0.48 | 0.072 |
| RA vs vehicle | 0.9 | 0.31 | 0.71 | 0.027 | 0.5 | 0.025 |

Table 2. Evaluation of the impact of ROL and RA application on concentration of TGM3 in the SC as evaluated by ELISA assay. Ratios of the concentration of TGM (versus vehicle) and *P*-value are given for each time point.

keratinocytes can be noticed on two levels. Firstly, an increased protein biosynthesis at early time points due to an upregulation of translation initiation factors (EIF6, EIF2S1, EIF4A1), the translation elongation factor (EEF2) and one 60S subunit of ribosome (RPLP2 (60S acidic ribosomal protein P2)). To our knowledge, this is the first report of retinoids' impact on protein translation which reflects the protein biosynthesis. In addition, this increase in protein production could potentially compensate for the decreased protein and polyamine biosynthesis in aged skin as demonstrated in previous studies²². Secondly, there were increased levels of CRABP2 and FABP5, retinoid binding proteins essential for carrying the RA to their nuclear receptors. In medulloblastoma, it has been shown that the levels of these retinoid binding proteins can lead to either proliferation when FABP5 levels are above CRABP2 levels as shown in our study or to growth inhibition (when CRABP2 > FABP5)^{23,24}. While both proteins were upregulated by the retinoids, FABP5 was found to be at higher increased levels than CRABP2, suggesting an increased proliferation. Furthermore, a positive effect on differentiation was observed at the level of keratin expression, with an upregulation of keratins 1 and 10, both well-known markers of terminal differentiation^{25,26}. Additionally, proteins of the epidermal differentiation complex including S100 proteins and FLG were found upregulated after ROL and RA application.

Several studies have also shown that skin aging is accompanied by significant changes in glycosaminoglycans (GAGs)²⁷ causing an alteration of their main functions as intercellular communication agents and as regulators of enzymatic activities. This might be linked to the glycan metabolic and catabolic pathways as GLB1 (galactosidase beta 1) is often found to be overexpressed in aged skin^{22,28}. In our study, 14 glycosidases involved in the de-glycosylation of several types of glycans were massively downregulated, suggesting the inhibition of shortening of GAGs by both retinoids. In particular, GLB1 and FUCA1 (Alpha-L-Fucosidase 1) were both consistently downregulated by the retinoids. This is to our knowledge the first report of such an important impact of retinoids on the modulation of the glycan degradation pathway. Interestingly, ROL seems to have a higher impact on the glycan degradation pathway as 5 additional glycosidases were regulated by ROL compared to RA in this study. This is probably due to the higher concentration of ROL compared with RA rather than a specific effect of ROL, since the conversion of retinol into retinoic acid is necessary to exert its cutaneous effects. Nevertheless, this interpretation highlights other works such as those by Kafi et al.²⁹ showing an increased expression of glycosaminoglycan after ROL treatment that might be through the modulation of enzymes from the glycosidase family and consistent with the parallel work of Donovan et al.³⁰ showing that modified glycan structure has been associated with aging.

While the proteomic analysis revealed the impact of ROL and RA on 2 new biological functions, we wanted to determine the impact of long-term topical application of retinoids on skin via the production of temporal *in vivo* signatures. The temporal *in vivo* signature obtained for the retinoids revealed the orchestrated molecular events that take place during long term retinoids application. Of the seven superpathways modulated by retinoid application, all functions were enriched at the three time points observed but with less DEPs over time. This observation would suggest that skin reaches an equilibrium after 12 months of treatment.

One of the biological functions for which the impact seems to be long lasting was epidermal barrier-associated proteins. The confrontation of proteomic data and morphological data (in vivo multiphoton microscopy data) shows that, as expected, molecular events precede morphological changes with a greater amplitude of proteins modulations at early times (M3 > M6-M12) whereas epidermal thickening is more significant at late times (M12 > M3-M6). As for the proteomic analysis, morphological modifications are modulated over time mainly with ROL with a significant epidermal thickening at M3 and M12 but not at M6. With RA, epidermal thickening was smaller and later, likely due to the high concentration of ROL used (0.3%), 12 times higher compared with RA concentration (0.025%) in this study¹⁰.

Some of the orchestrated events that can lead to epidermal thickening reside in the balance of proliferation/differentiation of keratinocytes *i.e.*, epidermal homeostasis. At 3 months of application, the balance in keratins implicated in keratinization was impacted with the up-regulation of KRT1 and KRT10 and down-regulation of KRT2 and KRT9. Keratin balance was modified again at 6 months with the upregulation of epithelial and basal layer keratins (KRT4, KRT5, KRT14). This shift was also supported by the upregulation of proteins precursors of the cornified envelope such as FLG, IVL, EVPL, PPL and KRTDAP, at the early time point of three months. While the impact of retinoids on keratin expression has been previously described^{31,32}, the kinetics of the retinoid signature in this study suggests a singularity in the shift between proliferation and differentiation with continuous application of retinoids. In addition, the molecular events leading to the keratinocyte's proliferation and thus the epidermal thickening requires a stepwise adaptation of the skin that can be detected as early as 3 months after retinoid application.

Similarly, orchestrated molecular events can be observed in protein biosynthesis, with an early upregulation of the initiation of translation (EIF2S1, EIF6 and EIF4A1 were upregulated at 3 months) followed by increased elongation process (EEF2 was upregulated at 6 months by RA and upregulated at 12 months by ROL). Once again, the orchestrated events highlighted the effect on protein biosynthesis and suggested an increased proliferation at early time points.

Conclusion

The strength of this study is the kinetics over one year, allowing a relevant analysis of the pleiotropic and complex effects of topical retinoids on skin, that are difficult to interpret at a single time.

The molecular signature of ROL and RA was produced using high throughput proteomics technology. To our knowledge, this is the most exhaustive proteomic signature produced to date revealing the effects of ROL and RA on skin's biological functions. In addition, we have shown that a simple non-invasive skin surface sample associated with a proteomic analysis enables to monitor the response to retinoids over time, opening the door to more personalized anti-aging treatment.

This study leads to highlight little or undescribed functions, in the mechanisms of action of ROL and RA including new function such as glycan shortening and proteins translation/biosynthesis. To go further, complementary *in vitro* or *in vivo* studies such as glycomics, metabolomics and protein turnover would be helpful to validate our new hypotheses. Furthermore, this new ROL signature could open the way to the selection of more powerful and better tolerated new anti-aging products.

Data availability

All data generated or analyzed during this study are included in this published article (and its supplementary information files).

Received: 9 March 2023; Accepted: 27 June 2023

Published online: 11 July 2023

References

1. Thomas, D. R. & Burkemper, N. M. Aging skin and wound healing. *Clin. Geriatr. Med.* **29**, xi–xx. <https://doi.org/10.1016/j.cger.2013.02.001> (2013).
2. Worley, C. A. Aging skin and wound healing. *Dermatol. Nurs.* **18**, 265–266 (2006).
3. Helbig, D. & Paasch, U. Molecular changes during skin aging and wound healing after fractional ablative photothermolysis. *Skin Res. Technol.* **17**, 119–128. <https://doi.org/10.1111/j.1600-0846.2010.00477.x> (2011).
4. Blair, M. J., Jones, J. D., Woessner, A. E. & Quinn, K. P. Skin structure-function relationships and the wound healing response to intrinsic aging. *Adv. Wound Care (New Rochelle)* **9**, 127–143. <https://doi.org/10.1089/wound.2019.1021> (2020).
5. Ma, J. *et al.* Quantitative proteomics analysis of young and elderly skin with DIA mass spectrometry reveals new skin aging-related proteins. *Aging (Albany NY)* **12**, 13529–13554. <https://doi.org/10.18632/aging.103461> (2020).
6. Kang, S. & Voorhees, J. J. Photoaging therapy with topical tretinoin: An evidence-based analysis. *J. Am. Acad. Dermatol.* **39**, S55–61. [https://doi.org/10.1016/s0190-9622\(98\)70446-3](https://doi.org/10.1016/s0190-9622(98)70446-3) (1998).
7. Baldwin, H. E. *et al.* 40 years of topical tretinoin use in review. *J. Drugs Dermatol.* **12**, 638–642 (2013).
8. Nyirady, J. *et al.* Tretinoin cream 0.02% for the treatment of photodamaged facial skin: A review of 2 double-blind clinical studies. *Cutis* **68**, 135–142 (2001).
9. Bellemere, G. *et al.* Antiaging action of retinol: From molecular to clinical. *Skin Pharmacol. Physiol.* **22**, 200–209. <https://doi.org/10.1159/000231525> (2009).
10. Tancrede-Bohin, E. *et al.* *In vivo* multiphoton imaging for non-invasive time course assessment of retinoids effects on human skin. *Skin Res. Technol.* **26**, 794–803. <https://doi.org/10.1111/srt.12877> (2020).

11. Bourassa, S. *et al.* Evaluation of iTRAQ and SWATH-MS for the quantification of proteins associated with insulin resistance in human duodenal biopsy samples. *PLoS ONE* **10**, e0125934. <https://doi.org/10.1371/journal.pone.0125934> (2015).
12. Yu, G., Wang, L. G., Han, Y. & He, Q. Y. clusterProfiler: An R package for comparing biological themes among gene clusters. *OMICS* **16**, 284–287. <https://doi.org/10.1089/omi.2011.0118> (2012).
13. Carbon, S. *et al.* AmiGO: Online access to ontology and annotation data. *Bioinformatics* **25**, 288–289. <https://doi.org/10.1093/bioinformatics/btn615> (2009).
14. Kanehisa, M. & Goto, S. KEGG: Kyoto encyclopedia of genes and genomes. *Nucleic Acids Res.* **28**, 27–30. <https://doi.org/10.1093/nar/28.1.27> (2000).
15. Michalik, L. & Wahli, W. Guiding ligands to nuclear receptors. *Cell* **129**, 649–651. <https://doi.org/10.1016/j.cell.2007.05.001> (2007).
16. Shaw, N., Elholm, M. & Noy, N. Retinoic acid is a high affinity selective ligand for the peroxisome proliferator-activated receptor beta/delta. *J. Biol. Chem.* **278**, 41589–41592. <https://doi.org/10.1074/jbc.C300368200> (2003).
17. Blatt, T. *et al.* Stimulation of skin's energy metabolism provides multiple benefits for mature human skin. *BioFactors* **25**, 179–185. <https://doi.org/10.1002/biof.5520250121> (2005).
18. Lopez-Otin, C., Blasco, M. A., Partridge, L., Serrano, M. & Kroemer, G. The hallmarks of aging. *Cell* **153**, 1194–1217. <https://doi.org/10.1016/j.cell.2013.05.039> (2013).
19. Acin-Perez, R. *et al.* Control of oxidative phosphorylation by vitamin A illuminates a fundamental role in mitochondrial energy homeostasis. *FASEB J.* **24**, 627–636. <https://doi.org/10.1096/fj.09-142281> (2010).
20. Alatshan, A. *et al.* All-trans retinoic acid enhances both the signaling for priming and the glycolysis for activation of NLRP3 inflammasome in human macrophage. *Cells* <https://doi.org/10.3390/cells9071591> (2020).
21. Gilhar, A. *et al.* Aging of human epidermis: Reversal of aging changes correlates with reversal of keratinocyte fas expression and apoptosis. *J. Gerontol. A Biol. Sci. Med. Sci.* **59**, 411–415. <https://doi.org/10.1093/gerona/59.5.b411> (2004).
22. Kuehne, A. *et al.* An integrative metabolomics and transcriptomics study to identify metabolic alterations in aged skin of humans in vivo. *BMC Genomics* **18**, 169. <https://doi.org/10.1186/s12864-017-3547-3> (2017).
23. Zhang, S. *et al.* Differential CRABP-II and FABP5 expression patterns and implications for medulloblastoma retinoic acid sensitivity. *RSC Adv.* **8**, 14048–14055. <https://doi.org/10.1039/c8ra00744f> (2018).
24. Astrom, A. *et al.* Molecular cloning of two human cellular retinoic acid-binding proteins (CRABP). Retinoic acid-induced expression of CRABP-II but not CRABP-I in adult human skin in vivo and in skin fibroblasts in vitro. *J. Biol. Chem.* **266**, 17662–17666 (1991).
25. Rosenthal, D. S. *et al.* Changes in photo-aged human skin following topical application of all-trans retinoic acid. *J. Invest Dermatol.* **95**, 510–515. <https://doi.org/10.1111/1523-1747.ep12504718> (1990).
26. Rosenthal, D. S., Griffiths, C. E., Yuspa, S. H., Roop, D. R. & Voorhees, J. J. Acute or chronic topical retinoic acid treatment of human skin in vivo alters the expression of epidermal transglutaminase, loricrin, involucrin, filaggrin, and keratins 6 and 13 but not keratins 1, 10, and 14. *J. Invest Dermatol.* **98**, 343–350. <https://doi.org/10.1111/1523-1747.ep12499802> (1992).
27. Carrino, D. A., Sorrell, J. M. & Caplan, A. I. Age-related changes in the proteoglycans of human skin. *Arch. Biochem. Biophys.* **373**, 91–101. <https://doi.org/10.1006/abbi.1999.1545> (2000).
28. Hildebrand, D. G. *et al.* alpha-Fucosidase as a novel convenient biomarker for cellular senescence. *Cell Cycle* **12**, 1922–1927. <https://doi.org/10.4161/cc.24944> (2013).
29. Kafi, R. *et al.* Improvement of naturally aged skin with vitamin A (retinol). *Arch. Dermatol.* **143**, 606–612. <https://doi.org/10.1001/archderm.143.5.606> (2007).
30. Donovan, M. *et al.* N-Glycans are stratum corneum biomarkers of aging skin. *J. Invest. Dermatol.* <https://doi.org/10.1016/j.jid.2022.07.023> (2022).
31. Torma, H. Regulation of keratin expression by retinoids. *Dermatoendocrinol* **3**, 136–140. <https://doi.org/10.4161/derm.3.3.15026> (2011).
32. Virtanen, M., Torma, H. & Vahlquist, A. Keratin 4 upregulation by retinoic acid in vivo: A sensitive marker for retinoid bioactivity in human epidermis. *J. Invest. Dermatol.* **114**, 487–493. <https://doi.org/10.1046/j.1523-1747.2000.00901.x> (2000).

Acknowledgements

Authors are grateful to Nathalie Parent who contributed to the organization of the clinical study and to Mark Donovan for his critical reading of the manuscript.

Author contributions

K.Abed, A.Foucher and N.Cavusoglu= Wrote the main manuscript text. K.Abed = Analysed proteomics results, kinetics and identification of new functions of retinoids. N.Cavusoglu and D.Bernard contributed to the biological interpretation. E. Tancrede-Bohin= Wrote the clinical protocol and instigator of the clinical study. N.Cavusoglu= instigator of the proteomic study. All authors reviewed the manuscript.

Competing interests

The authors declare no competing interests.

Additional information

Supplementary Information The online version contains supplementary material available at <https://doi.org/10.1038/s41598-023-37750-5>.

Correspondence and requests for materials should be addressed to K.A.

Reprints and permissions information is available at www.nature.com/reprints.

Publisher's note Springer Nature remains neutral with regard to jurisdictional claims in published maps and institutional affiliations.



Open Access This article is licensed under a Creative Commons Attribution 4.0 International License, which permits use, sharing, adaptation, distribution and reproduction in any medium or format, as long as you give appropriate credit to the original author(s) and the source, provide a link to the Creative Commons licence, and indicate if changes were made. The images or other third party material in this article are included in the article's Creative Commons licence, unless indicated otherwise in a credit line to the material. If material is not included in the article's Creative Commons licence and your intended use is not permitted by statutory regulation or exceeds the permitted use, you will need to obtain permission directly from the copyright holder. To view a copy of this licence, visit <http://creativecommons.org/licenses/by/4.0/>.

© The Author(s) 2023